J Therm Anal Calorim (2011) 104:991–997
DOI 10.1007/s10973-010-1127-8

Effect of precompression on isothermal decomposition kinetics of pure and doped potassium bromate

V. M. Abdul Mujeeb · M. H. Aneesh · K. Muraleedharan · T. G. Devi · M. P. Kannan

Received: 24 July 2010 / Accepted: 25 October 2010 / Published online: 14 December 2010

Abstract Pure and doped samples of potassium bromate ($KBrO_3$) were subjected to precompression and their thermal decomposition kinetics was studied by thermogravimetry at 668 K. The samples decomposed in two stages governed by the same rate law (contracting square equation), but with different rate constants, k_1 (for a $\alpha \leq 0.45$) and k_2 (for $\alpha \geq 0.45$), as in the case of uncompressed samples. The rate constants k_1 and k_2 decreased dramatically on precompression, the decrease being higher for doped samples. Cation dopants (Ba^{2+}, Al^{3+}) caused more desensitization effect than the anion dopants (SO_4^{2-}, PO_4^{3-}) of the same magnitude of charge and concentration. The results favor ionic diffusion mechanism proposed earlier on the basis of doping studies.

Keywords Decomposition mechanism · Doping · Ionic diffusion · $KBrO_3$ · Precompression

Introduction

In material science research, solid state decomposition studies are of paramount importance [1–4]. Solid state kinetic data are of practical interest for the large and growing number of technologically important processes. A number of reviews are available in the literature on these processes [5–9]. Many recent studies on the thermal decomposition of inorganic solids have included measurements on samples that were subjected to various pretreatments such as doping, preheating, crushing, irradiation, precompresion, etc., with a view to investigating their effects on the subsequent thermal decomposition. Pretreatments, for instance, can modify one or more properties of the material in an important way by generating imperfections, and thereby altering the number of nucleation sites in the solid. The nature of influence of pretreatments provides valuable information on the elementary steps and thereby on the mechanism and control of the solid state reactions [10–12].

Thermogravimetry (TG)—isothermal or nonisothermal - has been liberally used to obtain thermal stability parameters of solids [13–19]. It has been reported [17] that the popular model fitting approach gives excellent fits for both isothermal and nonisothermal data for the thermal decomposition of HMX and ammonium dinitramide, but yields highly uncertain values for Arrhenius parameters when applied to nonisothermal data, implying better reliability for isothermal methods.

As a part of our study of the effect of various pretreatments on the thermal behavior of high energy solids, we have examined the isothermal decomposition of $KBrO_3$ [20] as a function of small concentrations of the dopants, SO_4^{2-} and Ba^{2+}, by isothermal thermogravimetry in the temperature range 668–683 K. The results suggested a diffusion-controlled mechanism for the decomposition of $KBrO_3$, the diffusing species being both K^+ and BrO_3^-.

Whereas doping introduces point defects such as vacancies, interstitials, and impurity atoms in the solid, compression generates active dislocations and grain boundaries due to plastic deformation caused to the solid. Several authors [10, 11] have observed a drastic increase in the rate of decomposition of such precompressed solids due to the increased concentration of active sites where nuclei

V. M. Abdul Mujeeb · M. H. Aneesh · K. Muraleedharan · T. G. Devi · M. P. Kannan (✉)
Department of Chemistry, University of Calicut, Calicut 673 635, Kerala, India
e-mail: mpkannan@gmail.com

germinate and grow. However, compression can also cause densification of powdered materials as has been shown in many oxides [21]. The diffusion of atoms or ions will be obstructed significantly in a densified solid matrix. We, therefore, speculated that the rate of thermal decomposition of $KBrO_3$ would be lowered on precompression, if ionic diffusion determines the decomposition rate. Preliminary study with pure $KBrO_3$ [22] indicated in favor of this speculation. We have extended the study to doped samples of $KBrO_3$, and in this article, we report some interesting results that emphasize the importance of ionic diffusion in $KBrO_3$ decomposition.

Experimental

All the chemicals used were of AnalaR grade reagents of E Merck. Pure and doped samples of $KBrO_3$ were prepared by the method described earlier [20]. Precompression of $KBrO_3$ samples was carried out on a hydraulic pelletizing press. About 200 mg of the sample in the powder form (particle size: 90–106 μm) was taken in a stainless steel disc and then compressed to the required pressure up to a time of about 1 min. The pellet was taken out and lightly ground in an agate mortar and the particle size was again fixed in the same range, 90–106 μm to keep the external surface of the pressed and unpressed samples constant. Samples pressed in the range, 2×10^3 to 14×10^3 kg cm^{-2}, were used for the study. Similarly, $KBrO_3$ samples doped with SO_4^{2-}, PO_4^{3-}, Ba^{2+} and Al^{3+} at dopant concentrations 10^{-4} and 10^{-1} mol% were also subjected to compression at hydrostatic pressures of 2×10^3 and 14×10^3 kg cm^{-2}. All samples were stored in a desiccator over anhydrous calcium chloride. Thermal analysis of the precompressed samples was always done on the same day of the pretreatment in order to avoid the possible ageing effect.

Thermogravimetric measurements of all the samples were carried out in static air on a custom-made thermobalance fabricated in this laboratory [23], which is an upgraded version of Hooley [24]. A major problem [25] of the isothermal experiment is that a sample at room temperature requires some time to reach the furnace/decomposition temperature. During this short period of non-isothermal heating, the sample undergoes preheating/decomposition under uncontrolled temperature ramp producing data unsuitable for isothermal kinetic analysis. So we fabricated a thermobalance particularly for isothermal studies, in which loading of the sample is possible at any time after the furnace has attained the desired reaction temperature. The operational characteristics of the thermobalance are, balance sensitivity: $\pm 1 \times 10^{-5}$ g, temperature accuracy: ±0.5 K, sample mass: 5×10^{-2} g, particle size: 90–106 μm and crucible: platinum. Comparative runs were always made using samples of same age and particle size. The fraction of solid decomposed (α) was measured as a function of time (t) at 668 K.

Results and discussion

Figure 1 compares the α–*t* curves of the decomposition of uncompressed and precompressed samples of pure and doped $KBrO_3$ at 668 K (only selected points are shown in the figure to avoid overcrowding). The curves of compressed samples of $KBrO_3$ fall well below the uncompressed samples indicating clearly that the decomposition of both pure and doped samples was significantly suppressed by precompression.

Our study [20] on the effect of dopants on the thermal decomposition kinetics of pure $KBrO_3$ showed that no single equation fitted the whole α–*t* curve with a single rate constant throughout the reaction. In fact, the decomposition proceeded through two stages: a slow reaction ($\alpha = 0.15$–0.45) described by *contracting square equation* $[1 - (1 - \alpha)^{1/2} = kt]$ with rate constant k_1 and activation energy $E_1 = 216$ kJ mol^{-1}, followed by a faster reaction ($\alpha = 0.45$–0.95) described by *contracting square equation* itself, but with a larger rate constant k_2 and activation energy $E_2 = 276$ kJ mol^{-1}. The rate law envisages two-dimensional phase boundary reaction. The higher rate (k_2) for stage-2 process was suggested to be due to the mixing of $KBrO_3$ with the decomposition product KBr leading to auto catalysis and partial melting. Doping did not affect

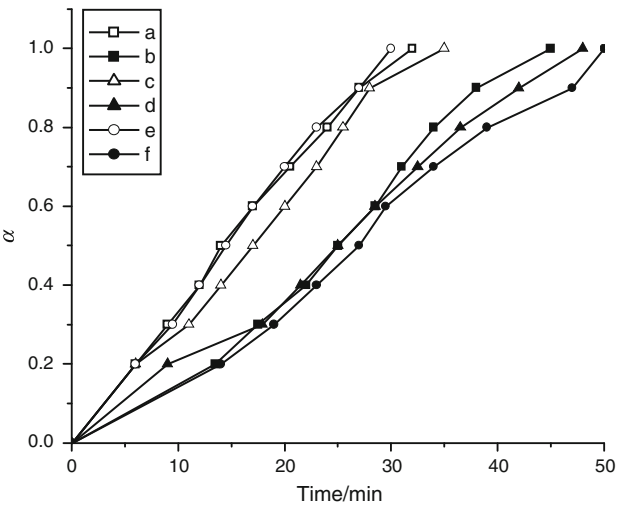

Fig. 1 Typical α–*t* curves for the thermal decomposition at 668 K of uncompressed (UC) and precompressed (C) samples of pure and doped (10^{-4} mol%) $KBrO_3$: *a* pure (UC), *b* pure (C), c. SO_4^{2-} doped (UC), *d* SO_4^{2-} doped (C), *e* Ba^{2+} doped (UC), and *f* Ba^{2+} doped (C)

either the rate law or the activation energy of these two stages of decomposition. The complex dependence of rates (k_1 and k_2) on the concentration and type of dopant ions suggested that diffusion of the similarly sized cation (K^+, 152 pm) and anion (BrO_3^-, 140 pm) [26] toward potential sites is the best possible rate-determining step of the decomposition; at the potential sites these ions undergo spontaneous reaction producing highly reactive radicals, which break down to form solid KBr and gaseous oxygen:

$$K^+ + BrO_3^- \rightarrow K^\bullet + BrO_3^\bullet \rightarrow KBr + 3/2O_2 \text{ (fast steps)}$$

The precompressed samples considered in this paper also decomposed through the same two stages described above for the uncompressed ones obeying the same rate law (*contracting square equation*) with separate rate constants k_1 and k_2. The values of k_1 and k_2 for the decompositions of precompressed samples of pure, anion (SO_4^{2-} and PO_4^{3-}) and cation (Ba^{2+} and Al^{3+}) doped samples of $KBrO_3$ at 668 K are given in Table 1.

Perusal of Table 1 reveals that both k_1 and k_2 decreased dramatically on precompression contrary to the increase observed with many solids, and that the decrease is more pronounced in doped samples. Besides, the higher the charge/concentration of the dopant ion, the higher is the magnitude of decrease in rates. The rate constants k_1 and k_2 reached their minimum values at a palletizing pressure of $\sim 2 \times 10^3$ kg/cm^2. Further increase in pressure did not show any considerable influence on the rate of decomposition, indicating a saturation of precompression effect in this solid. Figures 2, 3, 4, and 5 illuminate these features.

Solymosi [27] found that the decomposition of pure $KBrO_3$ (in the range 665–677 K) obeyed Prout–Tompkins equation with separate rate constants and obtained activation energies of 195 kJ mol^{-1} for $\alpha = 0.04$–0.46 and 173 kJ mol^{-1} for $\alpha = 0.50$–0.95. He also observed that the data in the range $\alpha = 0.30$–0.95 could be fitted to the first order rate equation with an activation energy of 191.6 kJ mol^{-1}. Diefallah et al. [28] found that under isothermal conditions the kinetics of the decomposition (in the temperature range 653–693 K) fitted the contracting square, the contracting cube or Avrami–Erofeyev ($n = 2$) equation, with an activation energy of 193.3 kJ mol^{-1} for the contacting cube model. Mohanty and Patnaik [29] reported that the decomposition of $KBrO_3$ consists of an initial slow first order reaction ($\alpha = 0.02$–0.26) followed by a fast first order reaction ($\alpha = 0.21$–0.98), but with the same activation energy, 218 kJ mol^{-1}. Isothermal decomposition of pure and doped (with SO_4^{2-} and Cl^-) $KBrO_3$ samples was carried out gasometrically in the temperature range 653–663 K by Das and Patnaik [30]. They observed that the kinetic data fitted well to the Prout–Tompkins and Avrami–Erofeyev mechanisms.

Generally, the initial region of a solid decomposition process is associated with the formation and growth of

Table 1 Rate constants for stage-1 (k_1) and stage-2 (k_2) decompositions of precompressed samples of pure, anion (SO_4^{2-} and PO_4^{-3}) and cation (Ba^{2+} and Al^{3+}) doped KBrO3 at 668 K

Dopant	Dopant concentration/mol %	Rate constant × 10^4/s^{-1}	Hydrostatic pressure × 10^{-3}/kg cm^{-2}						% Decrease in k at a hydrostatic pressure of 2×10^3 kg cm^{-2}
			0	2	5	8	11	14	
NIL	0	k_1	3.32	1.86	1.90	1.92	1.91	1.86	44
		k_2	5.13	5.00	4.94	4.97	4.89	4.88	19
SO_4^{2-}	10^{-4}	k_1	2.42	1.22	1.22	1.23	1.23	1.24	50
		k_2	5.78	3.19	3.22	3.21	3.20	3.20	45
	10^{-1}	k_1	2.84	1.24	1.25	1.26	1.27	1.28	56
		k_2	7.37	3.34	3.33	3.30	3.28	3.22	55
PO_4^{3-}	10^{-4}	k_1	2.27	1.07	1.08	1.10	1.11	1.12	53
		k_2	3.74	2.49	2.50	2.51	2.52	2.53	33
	10^{-1}	k_1	2.85	1.10	1.10	1.10	1.10	1.10	61
		k_2	5.62	2.52	2.51	2.51	2.51	2.50	55
Ba^{2+}	10^{-4}	k_1	2.93	1.25	1.25	1.25	1.25	1.25	57
		k_2	5.78	3.23	3.25	3.27	3.29	3.31	44
	10^{-1}	k_1	3.82	1.32	1.31	1.30	1.29	1.27	65
		k_2	6.47	3.25	3.25	3.26	3.27	3.28	50
Al^{3+}	10^{-4}	k_1	3.37	1.09	1.08	1.08	1.07	1.07	68
		k_2	6.09	2.50	2.50	2.51	2.50	2.51	59
	10^{-1}	k_1	5.18	1.11	1.08	1.08	1.07	1.07	79
		k_2	8.31	2.56	1.11	1.10	1.10	1.09	69

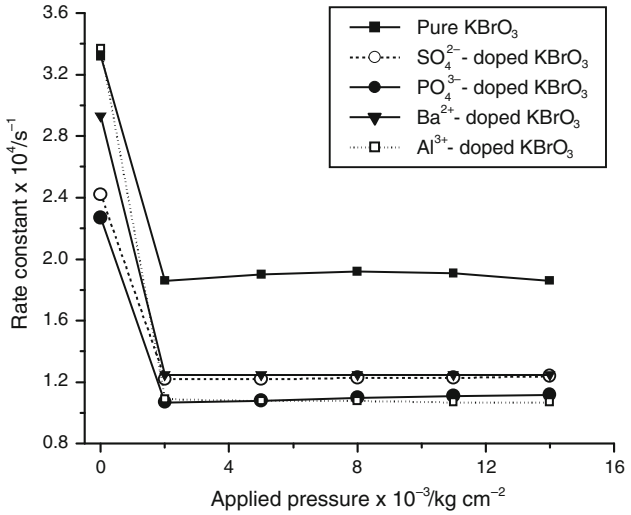

Fig. 2 Effect of precompression on the rate (k_1) of decomposition (668 K) of pure and doped (10^{-4} mol%) $KBrO_3$

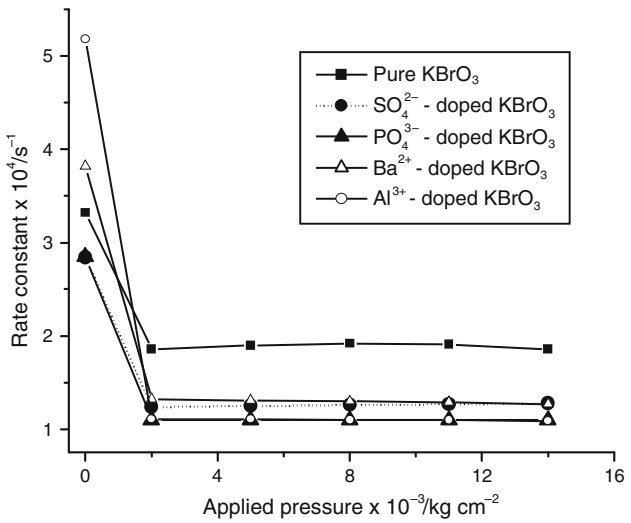

Fig. 3 Effect of precompression on the rate (k_1) of decomposition (668 K) of pure and doped (10^{-1} mol%) $KBrO_3$

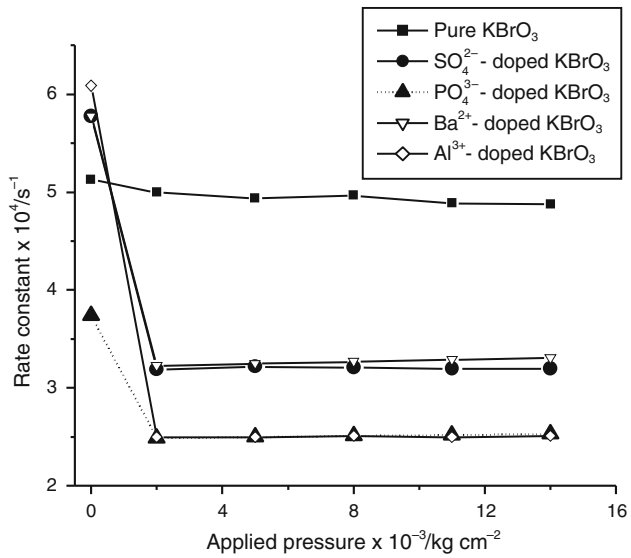

Fig. 4 Effect of precompression on the rate (k_2) of decomposition (668 K) of pure and doped (10^{-4} mol%) $KBrO_3$

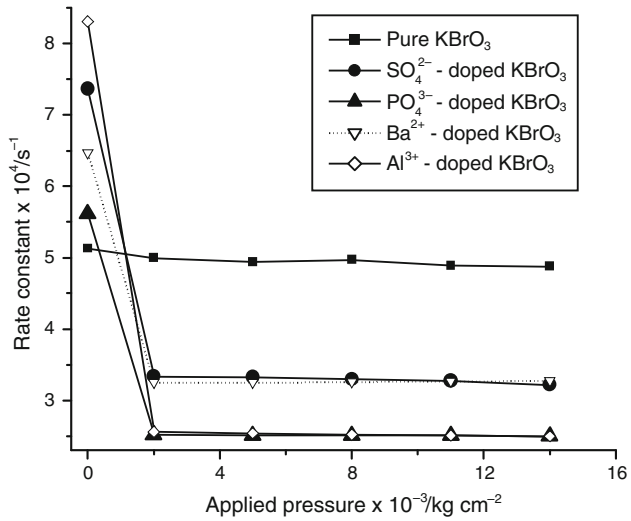

Fig. 5 Effect of precompression on the rate (k_2) of decomposition (668 K) of pure and doped (10^{-1} mol%) $KBrO_3$

nuclei and the final region with the decay of the growing nuclei as a result of their overlap. Thus, it is not unlikely that these two regions proceed with a single rate law and different rate constants or with different rate laws and different rate constants, as reported in the literature cited above. In this study, by model fitting method we found that both uncompressed and compressed samples of $KBrO_3$ decomposed following the contracting square law with two different rate constants.

On compression, a solid undergoes plastic deformation generating dislocations and grain boundaries, which are seats of high reactivity. X-ray and IR studies [11, 31, 32] have shown that compression resulted in an increase in the concentration of gross imperfections like dislocations in the crystal lattice and that the dislocation density increased with an increase in the pelleting pressure. Precompressed solids are generally known to decompose faster than the uncompressed samples due to the increased concentration of active sites where nuclei can germinate and grow [10, 11]. Compression is also known to cause sintering, and thereby densification of powdered materials as has been demonstrated in many oxides [21]. The inter-granular porosity is markedly reduced on compression, leading to densification of the solid. In an earlier work [22], we have observed that the rate of decomposition of NH_4ClO_4

(orthorhombic) and $KMnO_4$, which are known to decompose via electron transfer mechanism [33–36], increased significantly with increase in the precompression pressure. On the other hand, the decomposition rate of $KBrO_3$, which decomposes via ionic diffusion [20], spectacularly decreased on precompression (Note from Table 1 that k_1 is reduced by ~44% by the application of a hydrostatic pressure of 2×10^3 kg cm^{-2}). This suggests that the *densification effect* (rather than the *dislocation effect*) due to precompression can become crucial in systems that decompose through ionic diffusion mechanism, because the diffusion of ions will be obstructed significantly in a densified solid matrix. The movement of an electron from one ion to another, however, will not be noticeably affected by the densification by virtue of the extremely small size and high mobility of the electron compared with the ions, and the dislocation effect becomes decisive in such cases. Thus, it appears that the observed decrease in the rate of decomposition of precompressed $KBrO_3$ is a necessary consequence of the diffusion-controlled mechanism.

The above inference derives weight from the following behavior of doped $KBrO_3$. When a solid is compressed, both cation and anion vacancies coalesce causing great reduction in free space and hence densification of the solid matrix. Therefore, if ionic diffusion determines the rate, a crystallite containing a large number of lattice vacancies (cationic/anionic) should show a drastic decrease in its decomposition reactivity on precompression *irrespective of the 'type' of vacancies*. We thus speculated that $KBrO_3$ doped with multivalent cations or anions would show a significant decrease in the decomposition rate on precompression, if the rate is controlled by the diffusion of K^+ and/or BrO_3^-. Interestingly, this expectation was realized experimentally (Fig. 1; Table 1). Precompression caused significant decrease in the values of both k_1 and k_2 for cation as well as anion-doped samples of $KBrO_3$, despite the divergent actions of cation and anion dopants in generating vacancies. For instance, referring to Table 1 (last column), for a dopant concentration of 10^{-4} mol% and for an applied pressure of 2×10^3 kg cm^{-2}, the decrease in rate constant k_1 for samples doped with SO_4^{2-}, PO_4^{3-}, Ba^{2+} and Al^{3+} are ca. 50, 53, 57, and 68%, respectively, in contrast with the 44% decrease for pure $KBrO_3$; the % decrease in k_1 is higher for dopant concentration 10^{-1} mol%, as expected (see also Figs 2, 3). Similar effects are seen with k_2 also (Figs 3, 4). The results clearly demonstrate the higher susceptibility of the doped samples to densification, due to the larger *number* (and not the *type*) of vacancies present in them. Similar analysis of the data in Table 1 (last column), reveals the following important consequences of precompression:

(i) % decrease in rate for stage-1 decomposition ($\alpha = 0.15$–0.45) is higher than that for stage-2 in all cases.
(ii) % decrease in rate increases with increase in the charge of the dopants.
(iii) % decrease in rate increases with increase in the concentration of the dopants.
(iv) % decrease in rate caused by cation dopants is more than that caused by anion dopants of same magnitude of charge and concentration.

Stage-2 decomposition ($\alpha = 0.45$–0.95) involves $KBrO_3$ that has undergone decomposition to ~45%. The partial decomposition will leave the residue with free space making it less dense, facilitating the diffusion of the ions, which explains observation (i). The higher the magnitude of charge/concentration of the dopant, the higher the number of vacancies produced, and evidently, the higher will be the densification and the consequent desensitization effect if ionic diffusion controls the rate, which is in agreement with the observations (ii) and (iii). However, we note that the cation dopants cause more desensitization effect than the anion dopants of the same magnitude of charge and concentration even if the free space produced by each of them by generating vacancies is the same. For instance, with reference to k_1, SO_4^{2-} (size: 244 pm [26]) desensitizes the decomposition by ~50%, whereas Ba^{2+} (size: 149 pm [26]) desensitizes by ~57%, at a dopant concentration of 10^{-4} mol%. We suggest that this is due to the smaller ionic size of the cations which permits more number of them to enter the $KBrO_3$ lattice during cocrystallization, producing more vacancies. It may be noted that dopant concentration refers to the solution from which the dopant is cocrystallized [20].

It is well known that a solid is not easily compressed; it resists deformation. The isothermal compressibility of a solid ($\beta = -(dV/dP)/V$), which is a measure of the relative volume change of the solid with applied pressure, is generally small. Contreras-Garcia et al [37] have given a quantum chemical interpretation of compressibility of solids in terms of core, valence, bond, and lone electron pairs which fill the unit cell volume of solids. They conclude that cores are almost incompressible and do not contribute appreciably to the macroscopic compressibility, and lone pair basins are rather easier to compress than bond basins. Thus, as a solid is compressed progressively, interpenetration of orbitals occurs, but extreme electrostatic repulsive forces develop among the electrons preventing further compression beyond a certain applied hydrostatic pressure that is dependent on the electronic structure of the solid. We observe such a saturation of compression effect in pure and doped samples of $KBrO_3$ at

a hydrostatic pressure of $\sim 2 \times 10^3$ kg cm^{-2} (Table 1). Similar saturation was also observed [23] with $KMnO_4$ at $\sim 8 \times 10^3$ kg cm^{-2} and NH_4ClO_4 at $\sim 10 \times 10^3$ kg cm^{-2}, which indicates that among these three solids, $KBrO_3$ is least compressible and NH_4ClO_4 the most compressible. The fact that molar volume (=molar mass/mass density) of these solids, which is directly related to the unit cell volume, increases in the order, $KBrO_3 < KMnO_4 < NH_4ClO_4$, probably explains this trend.

Conclusions

This investigation demonstrates the powerful influence of precompression on the reactivity of $KBrO_3$ providing information to the solid state reactivity database. Precompression of $KBrO_3$ results in a dramatic decrease of thermal reactivity contrary to an usual increase observed with many solids (e.g., $KMnO_4$, NH_4ClO_4). Thus, $KBrO_3$ pellets would be thermally more stable than $KBrO_3$ powder. Invariability of the rate law (contracting square equation) on precompression suggests that the mechanism of decomposition of $KBrO_3$ is not affected by precompression, similar to doping [20]. The novel decrease observed in the rate of decomposition of $KBrO_3$ on precompression is suggested to be due to the *densification effect* of precompression rather than the *dislocation effect*, and appears to be characteristic of ionic diffusion-controlled reactions.

References

1. Galwey AK, Brown ME. Thermal decomposition of ionic solids. Amsterdam: Elsevier; 1999.
2. Vyazovkin S. Kinetic concepts of thermally stimulated reactions in solids: A view from a historical perspective. Int Rev Phys Chem. 2000;19:45–60.
3. Benderskii VA, Makarov DE, Wight CA. Chemical dynamics at low temperatures. New York: Wiley; 1994.
4. Brown ME, Dollimore D, Galwey AK. Reactions in the solid state comprehensive chemical kinetics, vol. 22. Amsterdam: Elsevier; 1980.
5. Brill TB, James KJ. Kinetics and mechanisms of thermal decomposition of nitroaromatic explosives. Chem Rev. 1993;93:2667–92.
6. Flynn JH. Thermal analysis. In: Mark HF, Bikales NM, Overberger CG, Menges G, editors. Encyclopedia of polymer science and engineering. New York: Wiley; 1989. p. 690.
7. Fatou JG. Crystallization kinetics. In: Mark HF, Bikales NM, Overberger CG, Menges G, editors. Encyclopedia of polymer science and engineering. New York: Wiley; 1989. p. 231.
8. Galwey AK. Is the science of thermal analysis kinetics based on solid foundations? A literature appraisal. Thermochim Acta. 2004;413:139–83.
9. Dollimore D. Thermal analysis. Anal Chem. 1996;68:63–72.
10. Herley PJ, Jacobs PWM, Levy PW. A photomicrographic and electron microscopy study of nucleation in ammonium perchlorate. Proc R Soc Lond. 1970;318A:197–211.
11. Pai Verneker VR, Rajeshwar K. Effect of prior mechanical and thermal treatment on the thermal decomposition and sublimation of cubic ammonium perchlorate. J Phys Chem Solids. 1976;37:63–6.
12. Lang A, Vyazovkin S. Effect of pressure and sample type on decomposition of ammonium perchlorate. Combust Flame. 2006;145:779–90.
13. Vecchio S, Rodante F, Tomasssetti M. Thermal stability of disodium and calcium phosphomycin and the effects of the excipients evaluated by thermal analysis. J Pharma Biomed Anal. 2000;24:1111–23.
14. Huang Y, Cheng Y, Alexander K, Dollimore D. The thermal analysis study of the drug captopril. Thermochim Acta. 2001;367:43–58.
15. Dollimore D, O'Connell C. A comparison of the thermal decomposition of preservatives using thermogravimetry and rising temperature kinetics. Thermochim Acta. 1998;324:33–48.
16. Halikia I, Neou-Syngouna P, Kolitsa D. Isothermal kinetic analysis of the thermal decomposition of magnesium hydroxide using thermogravimetric data. Thermochim Acta. 1998;320:75–88.
17. Vyazovkin S, Wight CA. Model-free and model-fitting approaches to kinetic analysis of isothermal and nonisothermal data. Thermochim Acta. 1999;340–341:53–68.
18. Rodante F, Vecchio S, Tomassetti M. Kinetic analysis of thermal decomposition for penicillin sodium salts: model-fitting and model-free methods. J Pharm Biomed Anal. 2002;29:1031–43.
19. Kotler JM, Hinman NW, Richardson CD, Scott JR. Thermal decomposition behaviour of potassium and sodium jasorite synthesized in the presence of methyl amine and alanine. J Therm Anal Calorim. 2010;102:23–9.
20. Kannan MP, Abdul Mujeeb VM. Effect of dopant ion on the kinetics of thermal decomposition of potassium bromate. React Kinet Catal Lett. 2001;72:245–52.
21. Budnikov PP, Ginstling AM. Principles of solid state chemistry: reactions in solids (trans: Shaw K). Maclarens and Sons Ltd., London; 1968. p. 244.
22. Kannan MP, Ganga Devi T. Effect of precompression on the thermal stability of solids. Thermochim Acta. 1997;292:105–9.
23. Kannan MP, Muraleedharan K. Kinetics of thermal decomposition of sulphate-doped potassium metaperiodate. Thermochim Acta. 1990;158:259–66.
24. Hooley JG. A recording vacuum thermobalance. Can J Chem. 1957;35:374–80.
25. Vyazovkin S, Wight CA. Kinetics in solids. Annu Rev Phys Chem. 1997;48:125–49.
26. Huheey JE. Inorganic chemistry principles of structure and reactivity. New York: Harper & Row Publishers; 1983.
27. Solymosi F. Structure and stability of salts of halogen oxyacids in the solid phase. London: Wiley; 1977.
28. Diefallah EM, Basahl SN, Obaid AY, Abu-Eittah RH. Kinetic analysis of thermal decomposition reactions: I. Thermal decomposition of potassium bromate. Thermochim Acta. 1987;111:49–56.
29. Mohanty SR, Patnaik D. Effects of admixtures of potassium bromide on the thermal decomposition of potassium bromate. J Therm Anal Calorim. 1989;35:2153–9.
30. Das BC, Patnaik D. Effect of anion doping on the thermal decomposition of potassium bromate. J Therm Anal Calorim. 2000;61:879–83.
31. Pai Verneker VR, Radhakrishnan Nair MN. Incomplete decomposition of ammonium oxalate. Combust Flame. 1975;25:301–7.
32. Pai Verneker VR, Kishore K, Kannan MP. Effect of pretreatment on the sublimation of ammonium perchlorate. J Appl Chem Biotechnol. 1977;27:309–17.
33. Bircumshaw LL, Newman BH. The thermal decomposition of ammonium perchlorate: i. Introduction, experimental, analysis of

gaseous products, and thermal decomposition experiments. Proc R Soc Lond. 1954;A227:115–32.
34. Maycock JN, Pai Verneker VR. Role of point defects in the thermal decomposition of ammonium perchlorate. Proc R Soc Lond. 1968;A307:303–15.
35. Kannan MP. Thermal decomposition of doped ammonium perchlorate. J Therm Anal Calorim. 1987;32:1219–27.
36. Boldyrev VV. Mechanism of thermal decomposition of potassium permanganate in the solid phase. J Phys Chem Solids. 1969;30:1215–23.
37. Contreras-Garcia J, Mori-Sanchez P, Silvi B, Recio JM. A quantum chemical interpretation of compressibility in solids. J Chem Theory Comput. 2009;5:2108–14.